Separation Science and Technology
Publication details, including instructions for authors and subscription information:
http://www.informaworld.com/smpp/title~content=t713708471

Desulfurization and Deashing of Solvent Refined Coal (SRC-I) by High Gradient Magnetic Separation Techniques

L. Petrakis[a]; P. F. Ahner[a]; F. E. Kiviat[a]
[a] GULF RESEARCH AND DEVELOPMENT CO. PITTSBURGH, PENNSYLVANIA

To cite this Article Petrakis, L. , Ahner, P. F. and Kiviat, F. E.(1981) 'Desulfurization and Deashing of Solvent Refined Coal (SRC-I) by High Gradient Magnetic Separation Techniques', Separation Science and Technology, 16: 7, 745 — 772
To link to this Article: DOI: 10.1080/01496398108058126
URL: http://dx.doi.org/10.1080/01496398108058126

SEPARATION SCIENCE AND TECHNOLOGY, 16(7), pp. 745–772, 1981

Desulfurization and Deashing of Solvent Refined Coal (SRC-I) by High Gradient Magnetic Separation Techniques

L. PETRAKIS, P. F. AHNER, and F. E. KIVIAT

GULF RESEARCH AND DEVELOPMENT CO.
PITTSBURGH, PENNSYLVANIA 15230

Abstract

A pilot-scale high gradient magnetic separations (HGMS) system was assembled to investigate the magnetic separation of ash-forming solids and inorganic sulfur from liquefied coal. The liquefied coal studied was a diluted intermediate product obtained from the DOE-sponsored Tacoma SRC-I pilot plant (50 t/d coal capacity). The magnetic characteristics and particle size distribution of the Tacoma SRC-I liquefied coal were optimized for removal by HGMS. The effect of the following magnetic separator parameters upon the deashing the desulfurization of the diluted liquefied coal was considered: matrix packing density, temperature, applied magnetic field, dilution of and residence time of liquefied coal feed, backflushing of saturated separator parameters upon the deashing and desulfurization of the diluted liquefied model which satisfactorily accounts for HGMS performance was developed. The HGMS system was observed to remove over 90% of the ash-forming materials and inorganic sulfur over a wide range of operating conditions. These removals were increased to 97 and 95%, respectively, with residence times greater than 6 min.

INTRODUCTION

Several coal liquefaction processes are under investigation, one of which is the *S*olvent *R*efined *C*oal-I (SRC-I) process. One of the objectives of this process is to produce a deashed, desulfurized, combustible product from coal.

The SRC-I process was developed at the DOE-sponsored Pittsburgh & Midway Coal Mining Co. SRC pilot plant (50 t/d coal capacity) in Tacoma, Washington (*1*). The process involves pulverizing raw coal and slurrying with a coal-derived solvent, referred to as process solvent, to yield a 30% by weight coal slurry. The slurry is fed with hydrogen to a dissolver at approximately 450°C and at a total pressure of approximately 10 MPa

(1670 psi). At this stage, most of the organic sulfur in the coal is removed as hydrogen sulfide, but the inorganic sulfur, undissolved coal, and ash-forming substances remain as solids. After the pressure is reduced, the slurry, which is referred to as filter feed, is passed through a rotary drum filter to remove the above solids at an average filtration rate of 0.3 gal filtrate per min per square foot of filter area. This last step has proved prone to problems due to filter design and operational difficulties.

Several researchers have done promising work that shows that coal could be deashed and desulfurized by the application of *H*igh *G*radient *M*agnetic *S*eparations (HGMS) (*2–7*). Liu and co-workers (*8–11*) at Auburn University, and Maxwell, Kelland, and co-workers (*12–18*) at Massachusetts Institute of Technology have applied HGMS to coal liquids from the Wilsonville, Alabama, SRC pilot plant (6 t/d coal capacity), a venture funded jointly by the Electric Power Research Institute and Southern Services. Liu and co-workers obtained an above 90% inorganic sulfur and a 75% ash reduction while the latter group obtained a 99% inorganic sulfur and a 40% ash removal. The MIT group also demonstrated that it is feasible to backwash adsorbed solids off the matrix.

The objective of the work reported here is to investigate the technical applicability of HGMS to the solid–liquid separation (i.e., inorganic sulfur and ash removal) in the Tacoma SRC-I filter feed. Since SRC-I product specification requires an ash content of less than 0.1% and a sulfur content of less than 1.0%, the ash removal must be essentially complete.

The following discussion considers the properties of the Tacoma SRC-I filter feed that indicate HGMS is a viable separations method for removing inorganic sulfur and ash, and also the effect of the systematic variation of the high gradient magnetic separator's operating conditions upon the separator's figures of merit, i.e., percent solids removal, percent ash removal, and percent inorganic sulfur removal. Also, a brief overview of HGMS phenomenology is presented in order to put the results in an appropriate perspective and define terms.

HIGH GRADIENT MAGNETIC SEPARATIONS

A number of detailed reviews of HGMS have appeared (*19, 20*). A typical high gradient magnetic separator consists of a pipe situated in the bore of a vertical solenoid magnet. The applied field is uniform along the vertical solenoid axis when the pipe is empty. The pipe is packed with a filamentary ferromagnetic matrix such as a stainless steel wool. High magnetic field gradients will exist in the applied field, with the gradients originating at filament edges, at surface imperfections, and near contact points between two or more filaments (*21*). Generally, for separators containing stainless steel wool matrices encountered in HGMS, the magnetic field gradients will

vanish at a distance from the filament gradient source similar in magnitude to the dimensions of that source (*19*). Thus the effect of the matrix is to create highly inhomogeneous magnetic fields at specific sites within the pipe.

Paramagnetic particles in an inhomogenous field experience an attractive force proportional to the product of the applied magnetic field and the gradient of the applied field while ferromagnetic particles experience an attractive force proportional solely to the gradient. Consequently, magnetic particles in a fluid flowing in the separator pipe will be attracted to filament sites from which a gradient originates provided they are in the domain of the gradient. This provides the basis for the HGMS separation, i.e., separation of magnetic particles from nonmagnetic fluid and/or particles.

Typical values of applied field magnitudes and gradients encountered in HGMS are approximately 2 T and 1×10^4 T/cm, respectively. Both the large field and field gradients result in weakly magnetic particles (i.e., paramagnetic particles with magnetic susceptibilities of approximately 10^{-6} to 10^{-8} emu/g) being attracted to the filament. Prior to the advent of HGMS, only strongly magnetic particles (i.e., ferro- and ferrimagnetic particles) could be removed by fields of 1 T for industrial processes (e.g., ore beneficiation). Strongly magnetic particles are, of course, attracted to the filament in a high gradient magnetic separator, in addition to the weakly paramagnetic particles.

The pertinence of HGMS to the deashing and desulfurization of coal liquids is that the ash-forming substance as well as the inorganic sulfur in coal is paramagnetic.

The major forces opposing the magnetic tractive force on particles are the hydrodynamic drag force and the gravitational force. The separation of paramagnetic particles from a nonmagnetic fluid will occur when the ratio of the magnetic tractive force to the sum of the opposing forces is greater than 1.

It has been shown (*19*) through the use of simplifying geometric assumptions, as well as assuming that all magnetic particles are spherical, that: (a) the magnetic tractive force acting on paramagnetic particles is directly proportional to the applied field intensity squared, the particle radius squared, and the difference between the particle and fluid susceptibilities; (b) the hydrodynamic drag force on a particle is directly proportional to the particle radius, fluid viscosity, and fluid velocity (and where flow is in the Stokes region); and (c) the gravitational force is proportional to the particle radius cubed. This illustrates the strong interaction between the properties of the particles (magnetic susceptibility, radius), the fluid in which the particles are suspended (viscosity, magnetic susceptibility), and the HGMS operating variables (feed velocity, field intensity, matrix, etc.) in determining separator performance. The effect of the above parameters on solids, ash, and inorganic sulfur removal from Tacoma SRC-I filter feed is now considered.

EXPERIMENTAL

The material investigated herein is Tacoma SRC-I filter feed obtained from liquefaction runs in which Kentucky #9 coal was slurried with process solvent. The coal has 9.0% ash (ASTM D271) and 3.3% sulfur (ASTM D2492), approximately half of which is in the form of pyrite. The process solvent is composed primarily of aromatics and is, therefore, diamagnetic. The filter feed as received from the Tacoma pilot plant had a solids content (weight percent) of 7.6%, 4.8% ash, and 1.03% sulfur. The runs reported herein, unless specified to the contrary, were performed using a Tacoma SRC-I filter feed further diluted with solids-free Tacoma SRC process solvent in the ratio 1:3. This further dilution proved necessary in order to maintain reasonable flow rates through the separator. The resultant HGMS feed contained (in weight percent) on the average 1.9% solids, 1.2% ash, and 0.61% sulfur.

The apparatus, procedures, and analytical methods used are as follows.

HGMS Apparatus

Figure 1 illustrates the apparatus used.

The separator is a SALA Magnetics, Inc. HGMS unit. It is capable of producing magnetic fields to 2 T in a volume of 15.2 cm length and 8.9 cm diameter in the solenoid bore. Contained within the solenoid bore is a removable canister.

The canister, which is wrapped in heating wire and asbestos tape, is made from Schedule 40 nonmagnetic 316 SS pipe 4.1 cm i.d. by 40.8 cm long. It is packed with Type 430 SS wool. In order to limit the amount of mechanical straining inevitably caused by the steel wool, the wool was replaced by spacers in the areas of the canister which were not magnetically activated. The wool-packed zone is bound on both ends by perforated disks to promote even flow distribution. Since only 15.2 cm of the wool matrix is magnetically activated, the true working volume is equal to that of a 15.2 cm (length) by 2.0 cm (radius) cylinder. Iron-constantan thermocouples were placed in the SRC flow path at both ends of the canister to obtain a true reading of SRC temperature.

Figure 1 also illustrates the flow scheme used. This feed system was designed to provide a nonpulsating upward flow of SRC through the separator. SRC was pressure-fed through the HGMS using the pressure in the feed tank and a flow restrictor to control the flow. Nonplugging flow restriction was accomplished by using various lengths of 0.068 cm i.d. stainless steel capillary tubes. Tube lengths between 3–80 cm and feed tank nitrogen pressures between 0.138–0.207 MPa (20–30 psi) were routinely

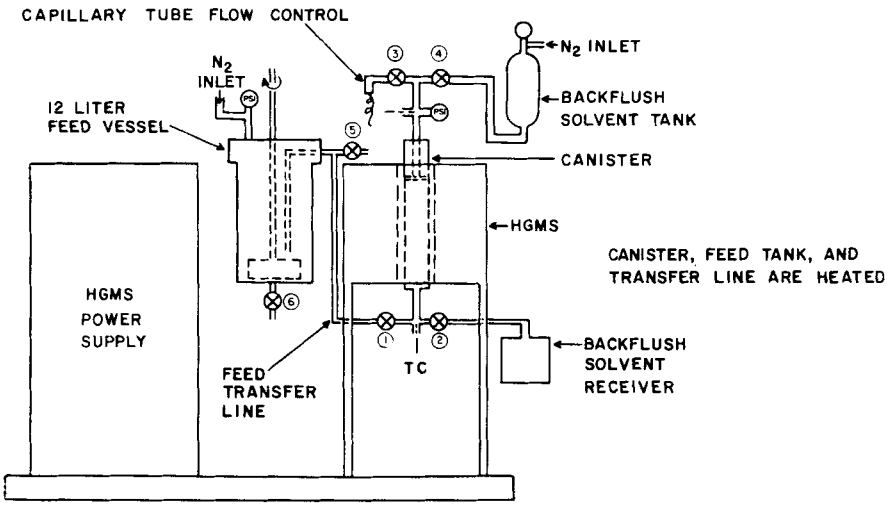

FIG. 1. HGMS apparatus.

used. The feed vessel was a Hastelloy B, 12-L autoclave, equipped with an air-driven stirrer. The feed transfer line extends close to the paddle-type stirrer to help assure uniform solids concentration in the feed.

Experimental Procedure

The experimental procedure was basically the same in all runs. The canister was packed with fresh steel wool prior to all runs. After the electrically heated canister and feed transfer line came up to temperature, the feed vessel was pressurized, the magnetic field turned on, and Valves 1 and 3 were opened to begin the experiment (Fig. 1). SRC temperature was monitored at the entrance and exit of the canister. Flow measurements were made throughout the run on a volume basis using graduated containers and a stopwatch. Flow and temperature generally became stable after the first 400 cc.

For the sake of greater accuracy, large samples (200 cc) of HGMS product were taken and filtered for suspended solids content. Four to six samples were taken during each run. In addition, a 75-cc sample was taken immediately after each 200 cc sample for other tests such as ash and sulfur. The feed was sampled through Valve 5. The flow rate was maintained to within $\pm 10\%$ by varying the nitrogen pressure in the autoclave. For those runs which contained a backflush cycle, the field was turned off and the backflush solvent was pressurized at the end of the run. Opening Valves 2 and 4 began the backflush (cleaning) cycle which stripped the steel wool of its

trapped SRC particles. Back pressure during the processing cycle generally remained below 0.034 MPa (5 psi).

Analytical Methods

The figures of merit used to describe the high gradient magnetic separator are: percent solids removal, percent ash removal, and percent inorganic sulfur removal. The necessary analytical tests to determine these parameters are suspended solids removal, ash analysis, and sulfur analysis. These analyses are as follows.

Suspended Solids Analysis

Analyses for percent suspended solids were carried out using a 142 mm Millipore pressure filter and Whatman No. 2 filter paper. Approximately 200 cc of sample was filtered in order to obtain a more accurate solids content on samples with low solids concentration. The percent deviation between identical samples was below $\pm 5\%$, with the majority below $\pm 3\%$.

A mixed cresol wash solvent was used to remove residual SRC from the trapped solids. Cresol was used in the first wash, since most other wash solvents cause precipitation of a carbonaceous residue when contacted with SRC. This residue would also be trapped by the filter paper, thereby leading to an unduly large solids content. After filtering the SRC sample, the filter cake was washed with three 100-cc aliquots of prefiltered mixed cresols and three 100-cc aliquots of toluene followed by a 1-h drying period at 100°C. The filter paper was cooled for 20 min before weighing.

The above filtration process proved to be quantitative in that a feed of 1.2% ash content yielded a filtrate having a 0.01% ash content.

Ash Analysis

Ash analyses were carried out on liquid samples collected immediately after the 200 cc sample was taken. Obtaining ash analyses on the liquid samples rather than the filtered solids made this test independent of the suspended solids analysis. Approximately 40 g of liquid were heated with a Bunsen burner until all of the combustible vapors burned off. The remaining solid carbon/ash mixture was then placed in a 815–838°C furnace until the sample weight remained constant. The ash was weighed after a 20-min cooling period. On samples with low solids content, a 60-g sample was ashed to increase accuracy. Percentage deviation generally ranged between 3–6% on identical samples.

Sulfur Analysis

Sulfur content was determined using a high temperature combustion method (ASTM D271–70) in a LECO sulfur analyzer. This method was used to analyze the liquid HGMS feed and product samples as well as the filtered solids. Due to the low sulfur content (0.6%) in the HGMS liquid feed, sulfur determination of HGMS liquid feed by this method was not reproducible. In cases where essentially all of the solids were removed from the liquid, complete inorganic sulfur removal was assumed. This was verified by the observation that the iron levels in the HGMS filtered liquid, as determined by atomic absorption, were identical to those in the process solvent (approximately 40 ppm).

PROPERTIES OF TACOMA SRC-I FILTER FEED

Two properties of the Tacoma SRC-I filter feed that are significant for solids removal by a high gradient magnetic separator are the particle size distribution and the magnetic susceptibility.

Elemental analysis of the Tacoma SRC-I filter feed solids yielded the following composition (weight percent): 30.5% carbon, 6.2% sulfur, 1.7% hydrogen, and 60.1% ash (*22*). The analysis indicates that portions of the coal remain undissolved by the liquefaction process. Coal itself is composed primarily of diamagnetic organic material with a susceptibility in the range -0.4×10^{-6} to -0.8×10^{-6} emu/g. The major ash-forming mineral species in coal are, with their susceptibilities (in 10^6 emu/g): quartz (−29), kaolins (20 to 29), iron sulfides (0.3 to 120), carbonates (−4 to 100), chlorides; and with the exception of quartz, all are paramagnetic (*3*). The liquefication process does not, in general, significantly alter the ash-forming mineral components, with the exception of the iron sulfides (*22*). The minerals do not dissolve in the process solvent, but rather, with some possible alteration, remain as solids.

Figure 2 illustrates the magnetization of the Tacoma SRC-I filter feed solids as a function of temperature (*22*). The peak magnetization occurs at 220°C. Qualitatively, Figure 2 is in agreement with previous thermomagnetic measurements performed on solids obtained from the Wilsonville SRC pilot plant coal liquids by Jacobs and Levinson (*14*). These authors found evidence for the reduction of the iron sulfide pyrite (FeS_2) to the ferrimagnetic pyrrhotite (Fe_7S_8) upon heating the solids to approximately 220°C. The ferrimagnetic pyrrhotite has a large magnetization and, therefore, its presence, even in relatively small amounts, can account for the increasing magnetization with increasing temperature. The decrease in the

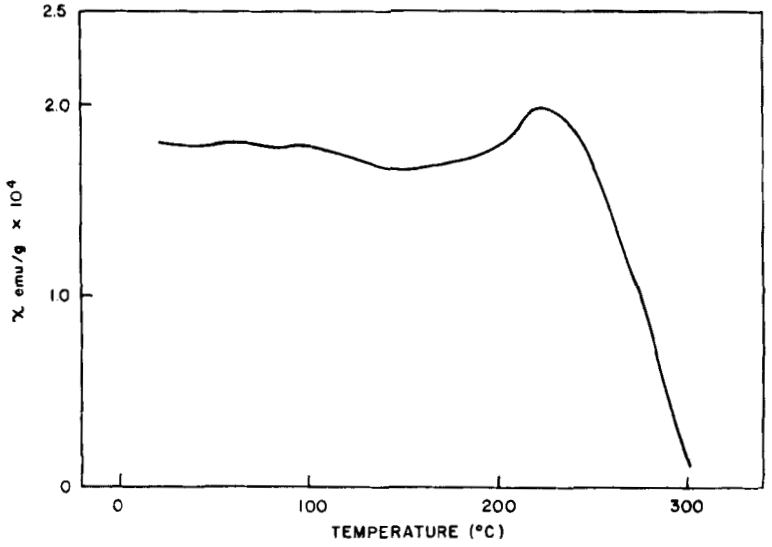

FIG. 2. Thermomagnetization of Tacoma SRC-I filter feed solids at 0.5 T.

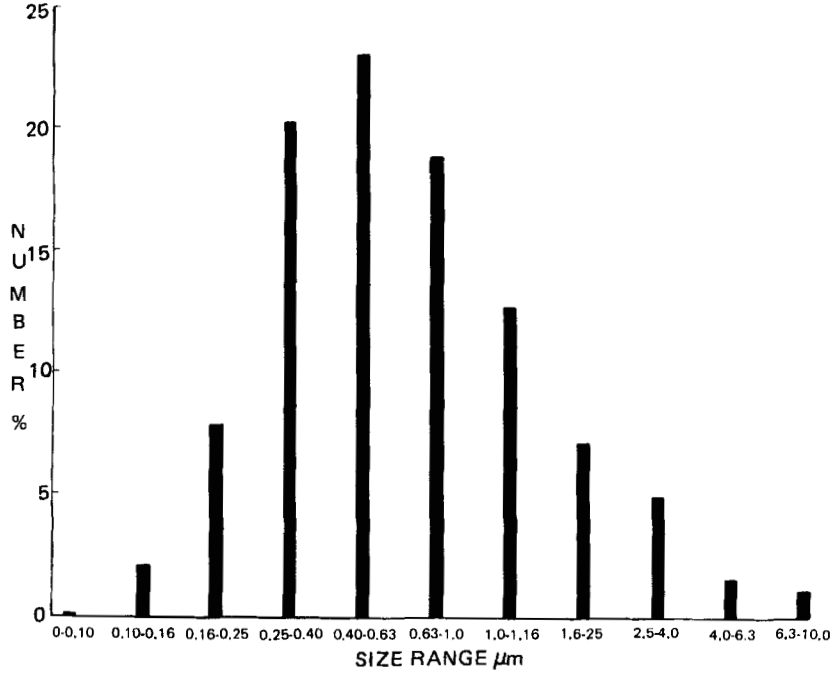

FIG. 3. Particle size distribution of Tacoma SRC-I filter feed solids.

magnetization beyond 230°C is attributed, in part, to the thermodynamic unstability of the ferrimagnetic pyrrhotite beyond this temperature. In this work the reversible temperature dependence was not studied, but we expect that it should be similar to the behavior reported by Jacobs and Levinson (*14*). The magnetic behavior presented in Fig. 2 shows that the Tacoma SRC-I filter feed solids possess suitable magnetic characteristics at temperatures less than 300°C for removal from the diamagnetic process solvent-dissolved coal system by means of a high gradient magnetic separator.

Figure 3 presents the particle size distribution (on a count basis) of the Tacoma SRC-I filter feed solids (*22*). Oberteuffer (*19*) has shown that the ratio of the magnetic tractive force to the sum of the opposing forces is maximized when the filament diameter is approximately three times the particle diameter. The mean particle diameter of the Type 430 stainless steel wool filaments is 24 μm.

If it is assumed that the filter feed particles are spherical and that the density of the particles is independent of their size, then approximately 75% of the weight of the Tacoma SRC-I filter feed solids comprises particles possessing diameters in the range of 10 to 16 μm. The mean particle diameter of the Type 430 SS wool is 24 μm. Therefore, on a weight basis, the filter feed particle size and Type 430 SS wool filaments are matched such that near optimal separation is anticipated.

A third property of the SRC-I filter feed that is significant in HGMS is the viscosity. However, it proved impossible to obtain reproducible viscosity data for the slurry using standard viscometers.

EFFECT OF SEPARATOR OPERATING CONDITIONS ON PERFORMANCE

The separation process is significantly dependent upon the manner in which it is performed (i.e., upon the process variables). The process variables which can be readily controlled in a high gradient magnetic separator are: the density of the stainless steel wool matrix, the feed velocity into the separator, the magnitude of the applied field, the concentration of the solids in the feed, and the temperature at which filtration occurs. The following discussion considers the effect of these process variables upon separator performance, as well as the number of regenerative cycles that a separator can undergo without performance degradation. Herein, separator performance is plotted versus the amount of feed treated in terms of separator canister volumes for the various process variables. These plots are significant in that they indicate separator performance as a function of matrix capacity or loading. The practical implications are obvious.

Numerous runs were performed to illustrate the effect of process variables

on separator performance. The following sections give representative results; the complete data set is not presented. This was to limit the reduncancy in the reported results. Later, when a model is developed for separator performance, the entire data base is utilized.

Matrix Packing Density

Percent matrix packing density is defined as the weight of the steel wool packed in the canister divided by the weight of solid stainless steel required to fill the same canister volume multiplied by 100. Percent voids are obtained by subtracting percent packing density from 100.

The packing density of the matrix may be significant in determining the number of high gradient trapping sites produced. Too loose a packing will decrease the number of high gradient sites by reducing the contact or near contact between fibers and also by decreasing the concentration of sites originating from the wool fiber itself. With fewer trapping sites, the probability for particles to completely avoid high gradient originating sites is increased and the number amount of trapped particles a given matrix can hold (capacity) is reduced.

Figure 4 shows data comparing the percent solids removal at two matrix density levels. The matrix with lesser void space yields significantly better results than the more loosely packed matrix. Straining (zero field) runs made on both matrices yielded between 34 and 36% solids removal at about 9 canister volumes, indicating that relative removals were not affected appreciably by mechanical entrapment. Matrices are used with approximately 86–88% void space.

Effect of Flow Velocity

Since we are dealing with SRC particles, most of which have weak paramagnetic characteristics and, therefore, are not very strongly held, drag forces play a major role in HGMS performance. As mentioned before, drag force is directly proportional to fluid velocity.

Figures 5–7 contain data obtained at three different flow velocities under approximately the same experimental conditions. Flow velocities were obtained by dividing the volumetric flow rate (cc/s) by the cross-sectional area (cm^2) of the canister. Corresponding residence times were determined by dividing the matrix-void volume by the volumetric flow rate. Figure 5 (flow velocity = 0.17 cm/s) shows a region of consistently high solids/ash removal (95–98%) followed by a steeply sloping section in which removal falls off sharply. The straight line extrapolation of these two slopes forms an intersection (breakthrough point) at which it could be said that all of the

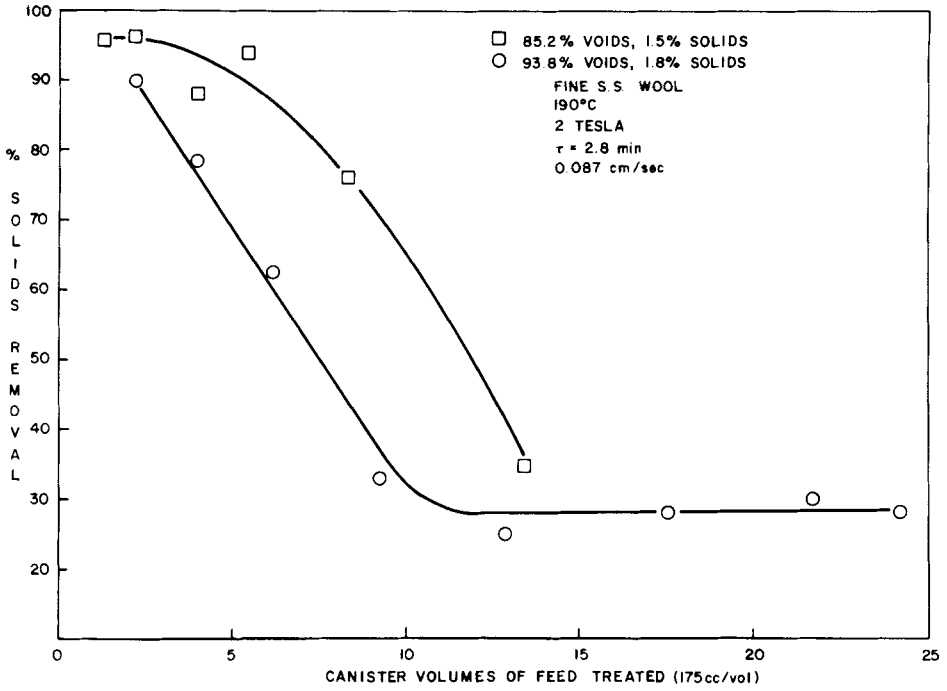

FIG. 4. Effect of matrix packing density upon separator performance.

ultralarge gradient sites capable of trapping most of the SRC particles are filled. From this point on only the more strongly paramagnetic particles are removed and/or the probability for particles to contact a magnetic site is decreased. The separator performance begins to degrade at the breakthrough point. The breakthrough point at this particular flow velocity is close to 15 canister volumes (175 cc/canister volume). The lower data, obtained from a straining (zero field) run, indicate approximately 37% solids removal due to mechanical filtering by the steel wool. Figure 6 shows data obtained at a slower velocity of 0.04 cm/s ($\tau = 6.1$ min). The drag force exerted on the trapped particles in this run should be approximately a fourth that of the former. An improvement in HGMS performance should therefore be expected. Although there is no significant improvement in the degree of solids/ash removal, the breakthrough point has been extended to at least 19 canister volumes, presumably due to the quartering of drag force afforded by the slower flow and the increased amount of straining occurring (43 vs 37%). Figure 7 shows the solids, ash, and sulfur removal efficiencies at the much higher flow velocity of 1.36 cm/s. At this high velocity the performance of the filter is poor in comparison to the slower rates (Figs. 5 and 6).

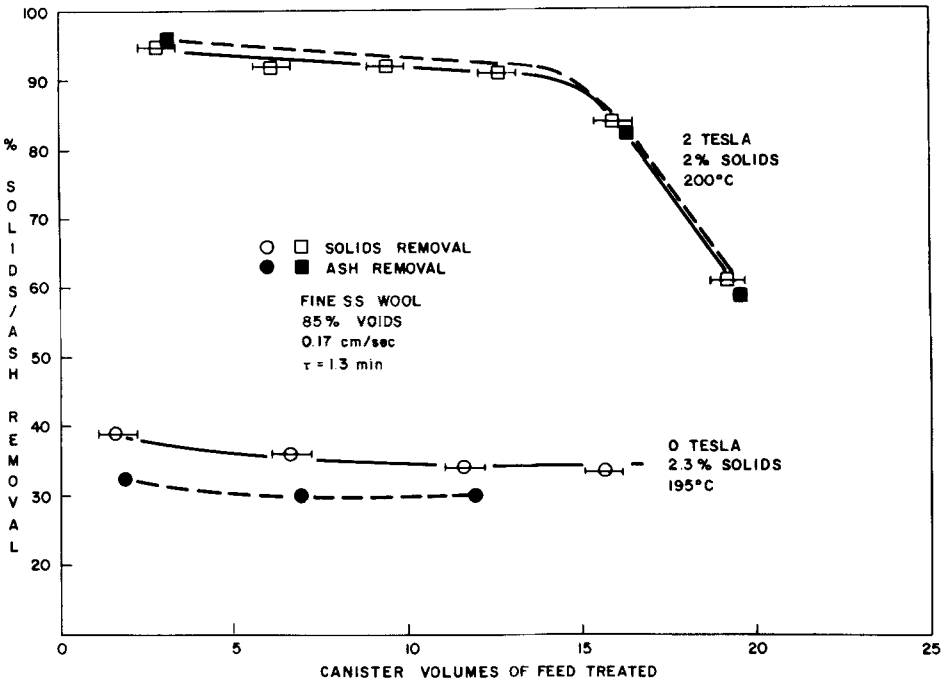

FIG. 5. Percent removal at 0.17 cm/s flow velocity. (The length of the bars represents the sample volumes.)

Using data in Figs. 5, 6, 7, and other runs in the data base, plots showing percent solids/ash removal versus flow velocity can be drawn at any point along the HGMS run (i.e., canister volumes of feed treated). Figures 8 and 9 contain plots made at 5, 10, 15, and 20 canister volumes of SRC processed using a feed containing approximately 2% solids (1.2% ash). These plots give a clear indication of the effect of fluid velocity upon HGMS performance. It is observed that at flow velocities of 0.2 cm/s or less, 90% removal occurs for an amount of feed equivalent to 15 separator volumes.

Effect of Field Strength

For trapping weakly paramagentic SRC particles, field strength should play a very important role. Decreasing field strength decreases the strength of the magentic moment induced in the SRC particle, thereby decreasing the tractive effect that high gradient sites can have on the particle. Furthermore, if field strength is reduced to below that required to saturate the steel wool fibers themselves, the number and intensity of high gradient sites will

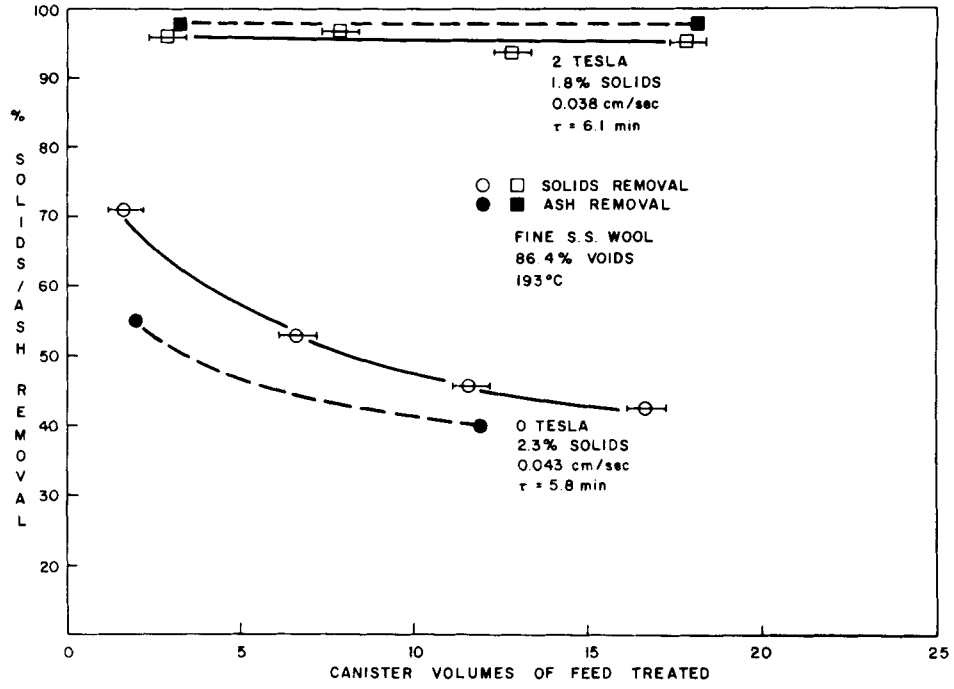

FIG. 6. Percent removal at 0.04 cm/s flow velocity.

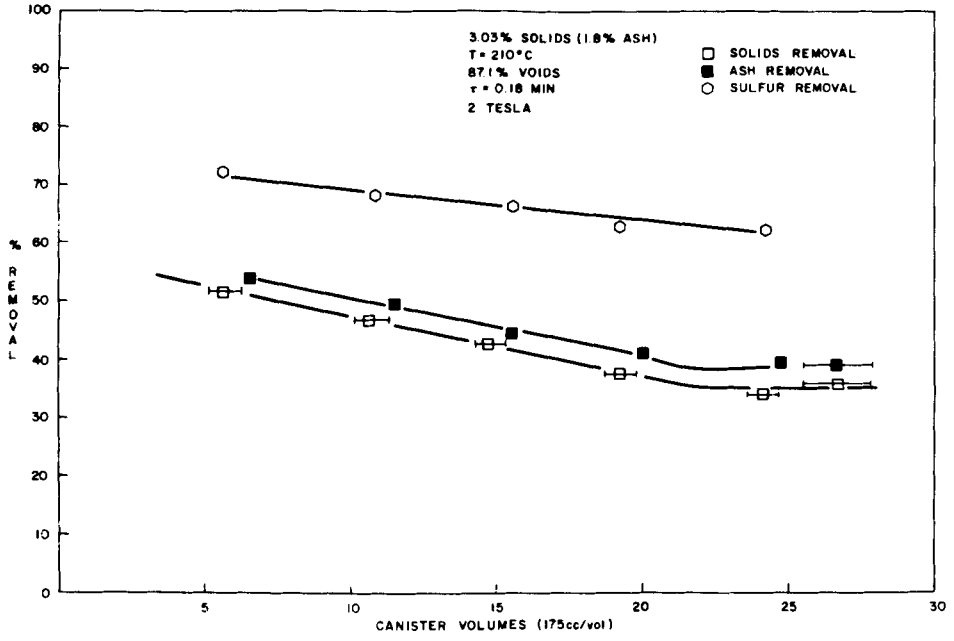

FIG. 7. Percent removal at 1.36 cm/s flow velocity.

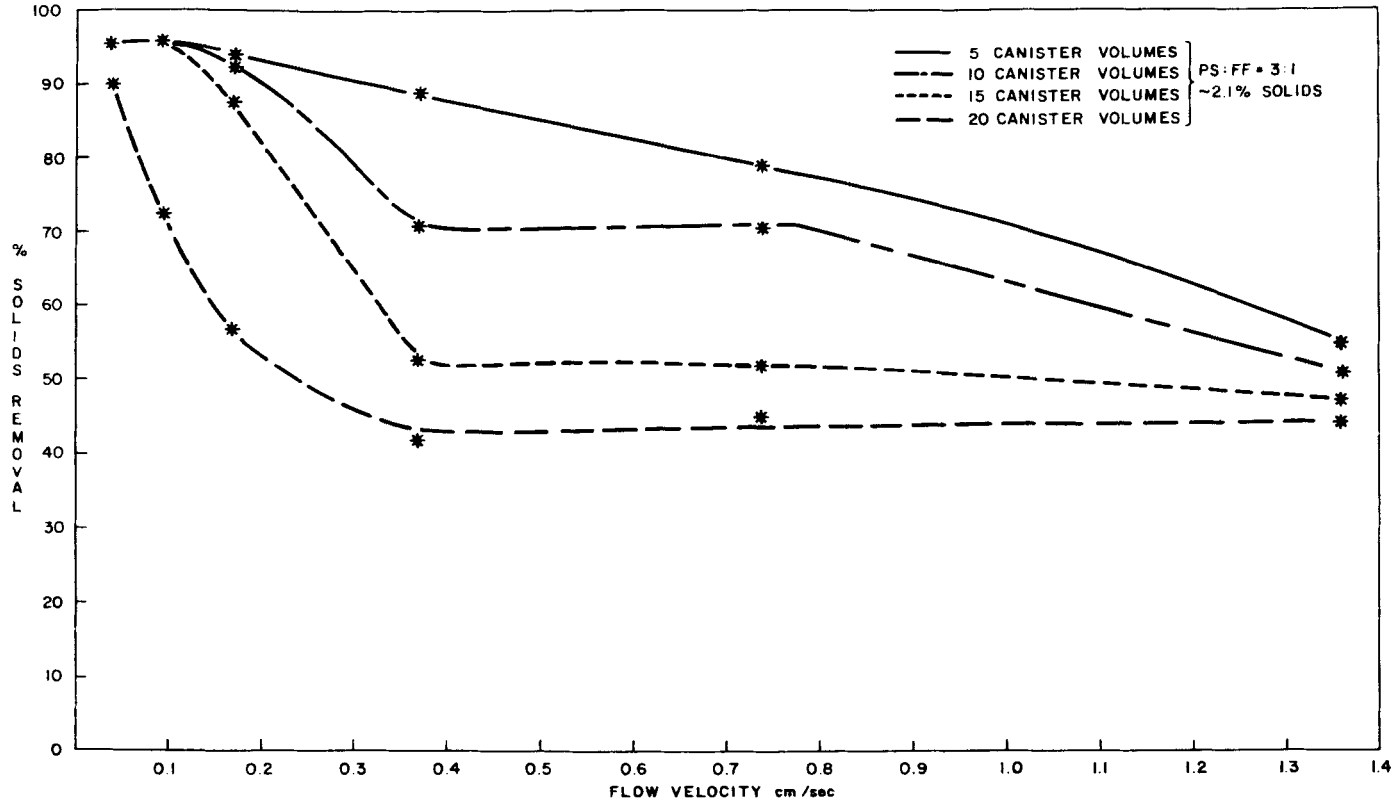

FIG. 8. Percent solids removal vs flow velocity at various volumes of feed treated.

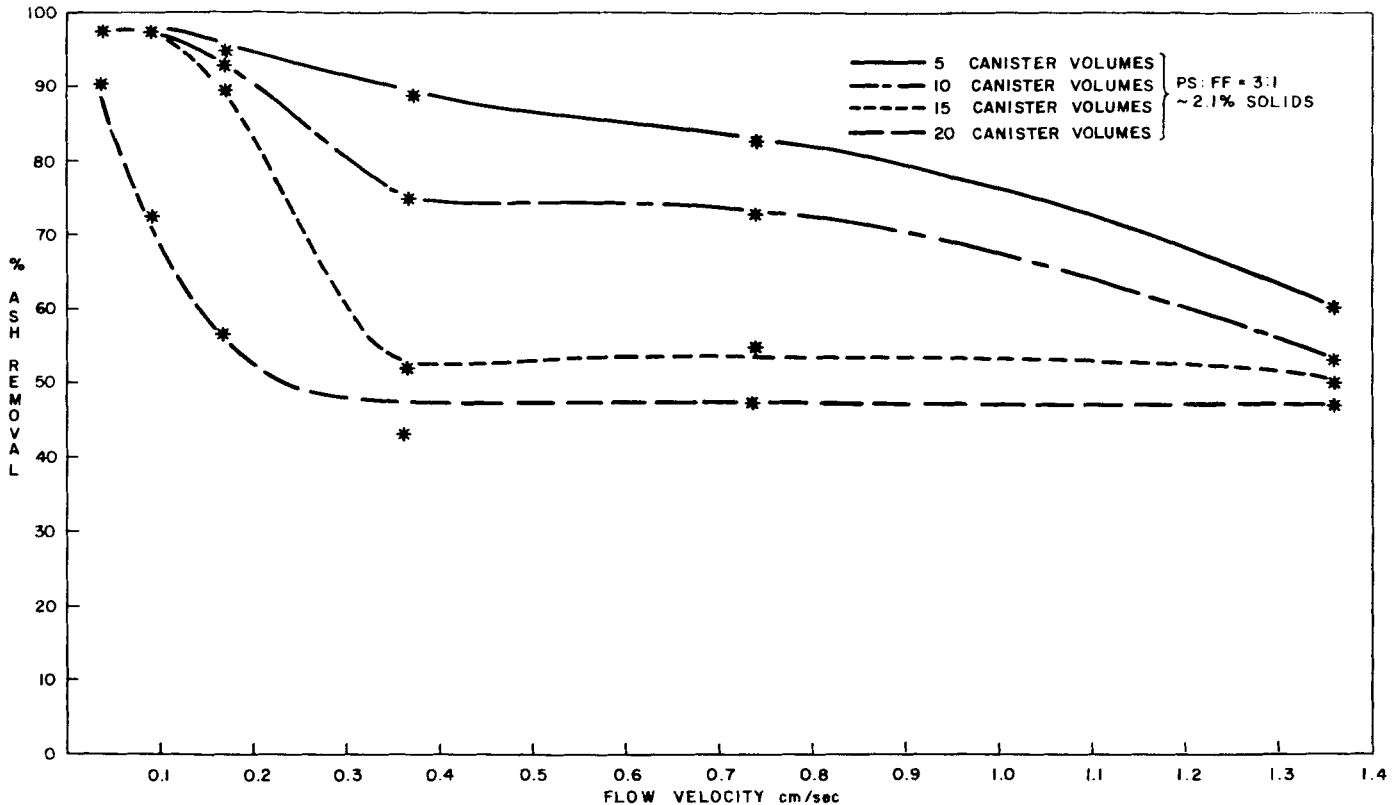

FIG. 9. Percent ash removal vs flow velocity at various volumes of feed treated.

decrease. Since field strengths remain above or close to the magnetic saturation value of the steel wool (0.8–0.9 T), the data obtained should mainly reflect induced magnetic dipole strength changes in the SRC particles.

Figures 10 and 11 contain percent solids/ash removal data at three different field strengths 2, 0.92, and 0 T, respectively. While the maximum degree of removal at both 2 and 0.92 T remains high (95–96%), the breakthrough point of the 0.92 T plot occurs much sooner (12.5 canister volumes) as compared with the 2 T plot (16 canister volumes). Percent removal also falls off much more sharply. The zero field plot simply shows data from a straining run with the same experimental parameters.

Effect of Dilution

All of the runs made up to this point involved a feed consisting of roughly one part SRC filter feed and three parts of process solvent. This mix was used

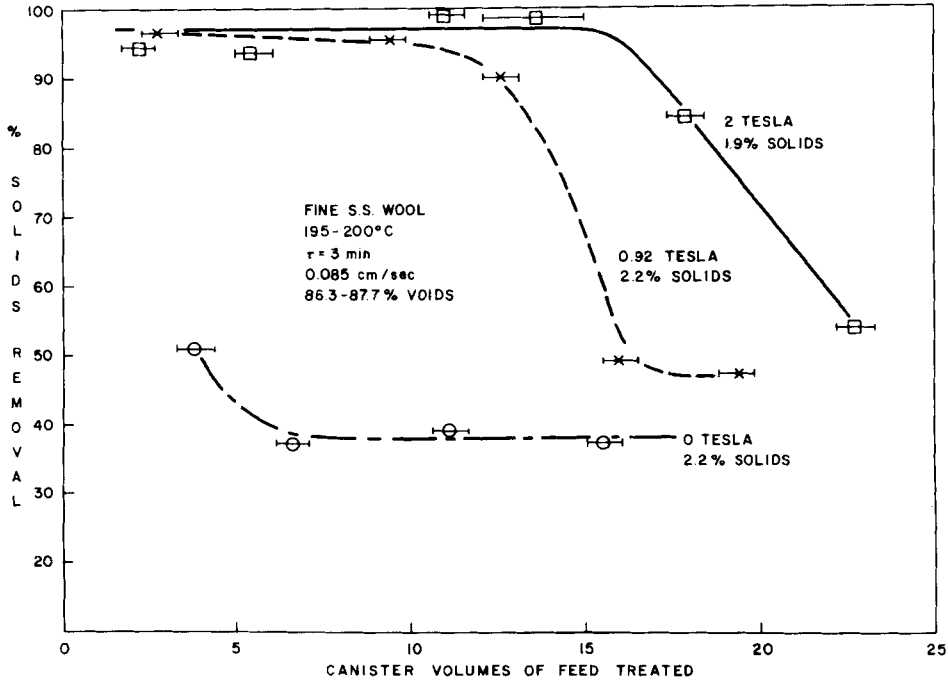

FIG. 10. Percent solids removal vs volume of feed treated at various field strengths.

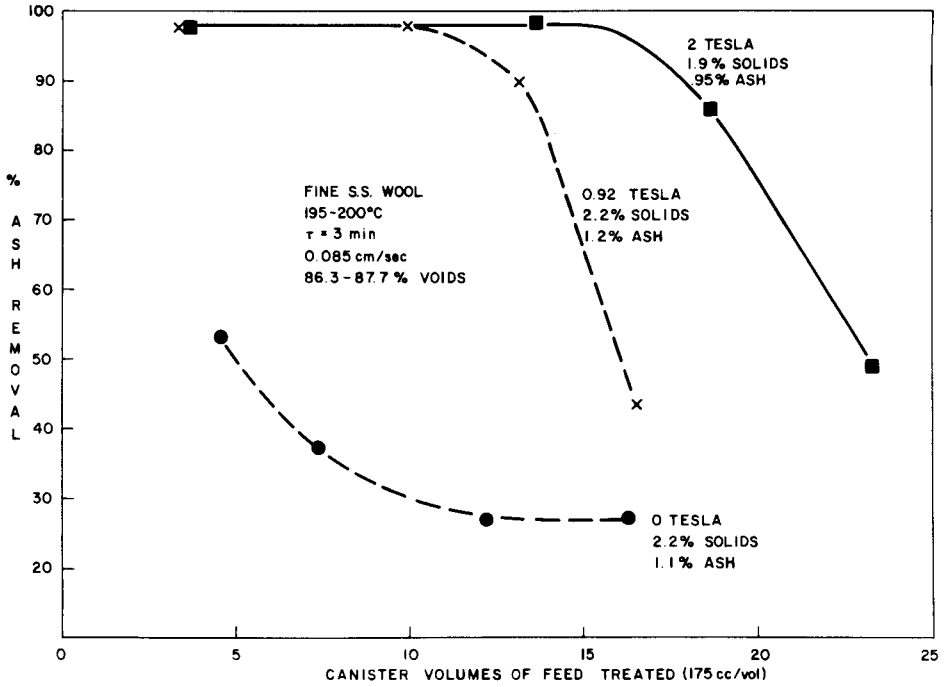

FIG. 11. Percent ash removal vs volume of feed treated at various field strengths.

to decrease the viscosity and the solids content of the feed. A run was made using a 1:2 filter feed process solvent mix in order to determine the effect of dilution. This change increased the solids content from approximately 2 to 3.2%. The data from this run are shown in Fig. 12. The other experimental parameters are nearly identical to those shown in Fig. 13 where solids content is approximately 2%, so a direct comparison can be made. The increased solids content of the feed did have a significant effect on HGMS performance and straining characteristics. While the percent removal data for both runs (1:2 and 1:3 runs) are comparable, the absolute quantities of solids and ash remaining in the 1:2 product are somewhat greater. For example, 94% removal in the 1:2 run and 1:3 run corresponds to 0.19% solids and 0.12% solids, respectively. The breakthrough point in the 1:2 run also occurred sooner, 13 cannister volumes versus 16 canister volumes in the 1:3 run. The earlier breakthrough point for the 1:2 run was expected, since the larger concentration of particles caused the high gradient trapping sites to be filled sooner. The absolute quantities of solids built up on the matrix at the breakthrough point of both plots are very similar.

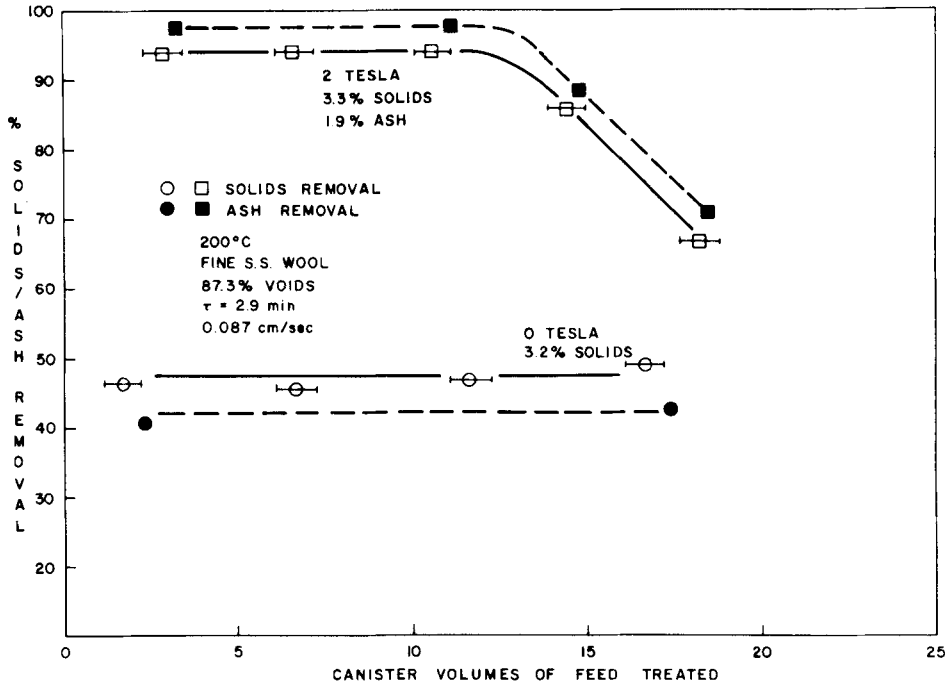

FIG. 12. Percent removal at 3.0% solids content of feed.

Effect of Temperature

Figures 13, 14, and 15 contain solids/ash removal versus canister volume at 190, 150, and 245°C, respectively. Straining runs (lower plots) were also made. As experienced with the field strength runs, the degree of removal was not affected by temperature. Percent solids/ash removal remained between 95–98% until the breakthrough point was reached. Temperature did affect the breakthrough point, however. At 150°C the breakthrough point occurred at approximately 14 canister volumes, whereas at 245°C the breakthrough point was extended to greater than 19 canister volumes. No doubt the increased straining occurring at 245°C (43% removal) versus 150°C (38% removal) also improved the higher temperature run.

Increasing the temperature from 150 to 245°C should have the effect of decreasing the hydrodynamic drag force by decreasing viscosity. The improved separator performance at the higher temperature is most probably due solely to a decrease in viscosity; the magnetic susceptibility of the Tacoma SRC-I solids does not vary significantly within this temperature range.

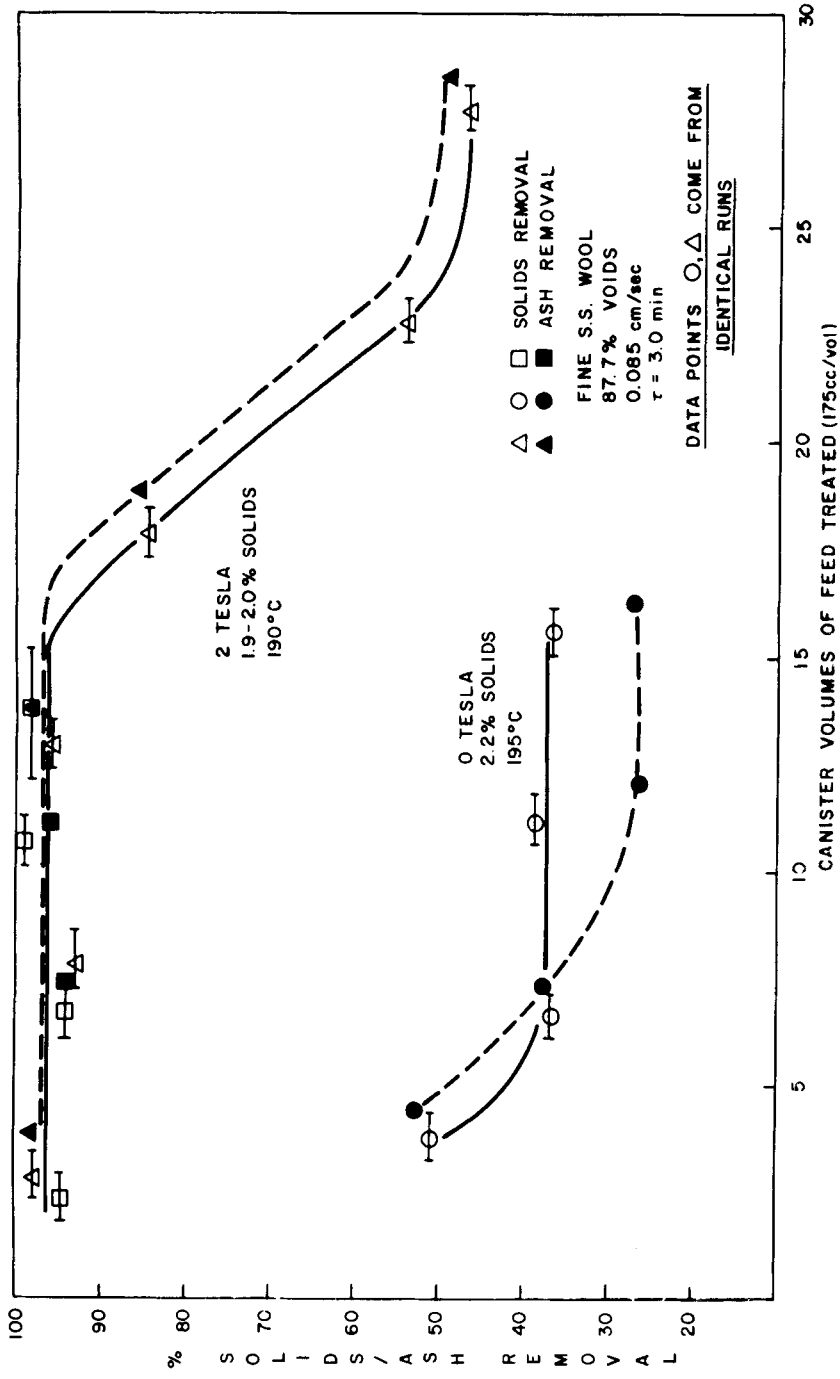

FIG. 13. Percent removal at 2.0% solids content of feed.

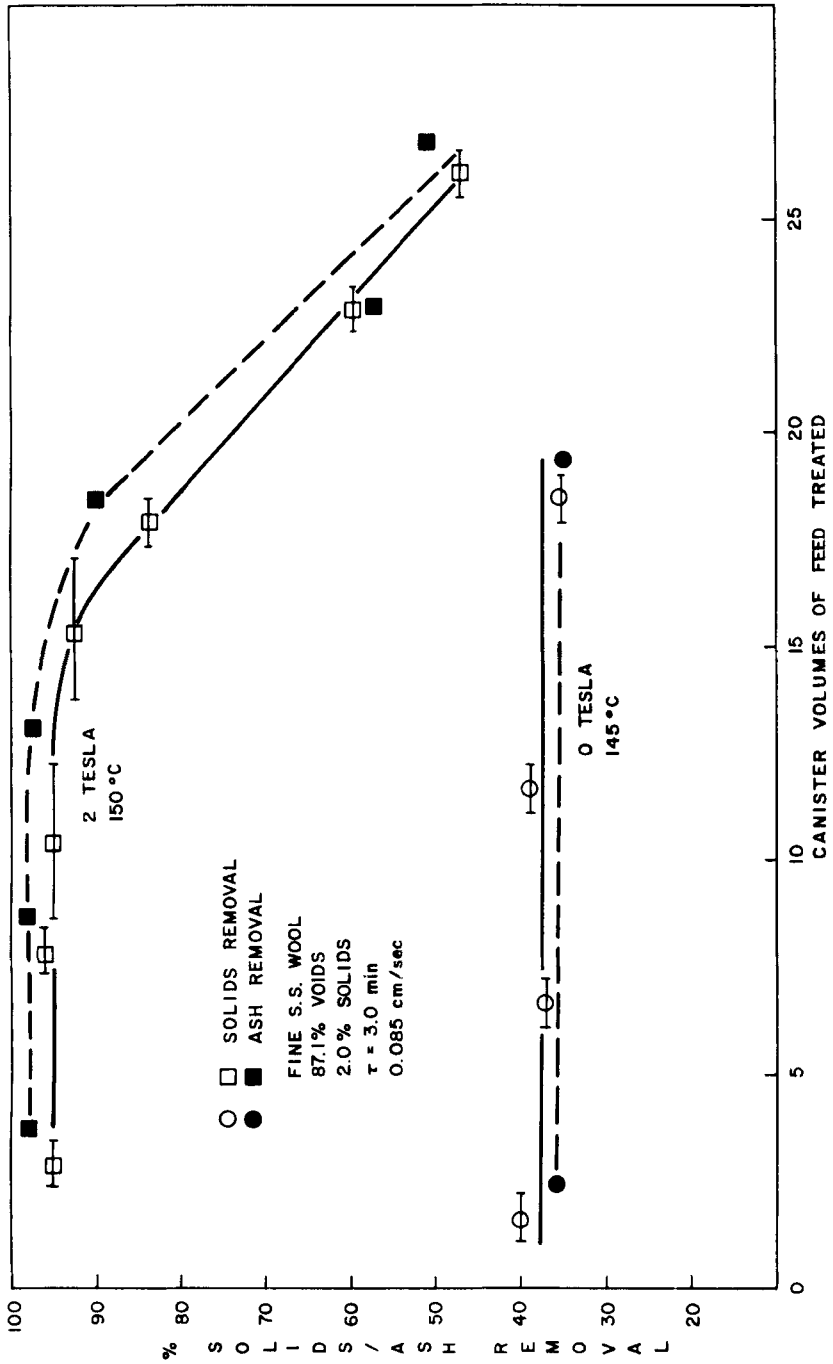

FIG. 14. Percent removal at 150°C.

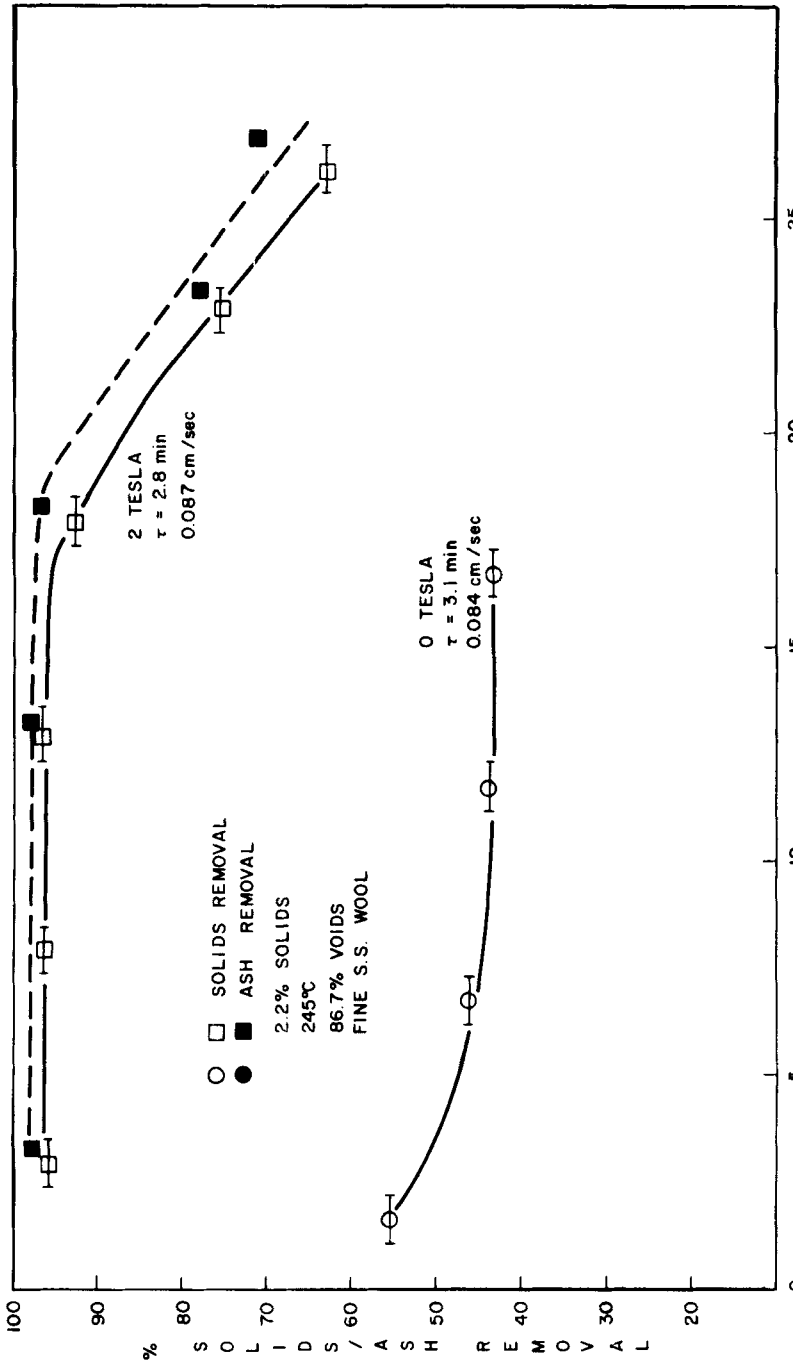

FIG. 15. Percent removal at 245°C.

Fresh Matrix Versus Backflushed Matrix

Except where specifically stated, all of the runs made up to this point involved a fresh stainless steel wool matrix; that is, the used wool was removed and replaced by new wool before each run. In most types of practical applications, constant replacement of the matrix would be prohibitively expensive. With this in mind, runs were made studying the effectiveness of an *in situ* matrix cleaning procedure. The procedure involved backflushing the matrix with cresol with the field off. Cresol flow velocity was 4.1 cm/s (47 cc/s) and the driving pressure was 1.0 MPa (167 psi). Viscosity of the cresol was also increased by allowing the matrix to cool to below 100°C before backflushing. The volume of backflush cresol was 700 cc (4 cannister volumes). The cresol flow was interrupted about five times during the backflush to provide a pulsating action. After the cresol, short blasts of nitrogen were used to blow the residual cresol out of the matrix prior to another run. Figure 16 follows a run through three backflush cycles. With fresh steel wool, a breakpoint at 16 canister volumes was observed, whereas the fourth cycle matrix yielded a breakpoint between 17 and 19 canister volumes. The reason for the better performance after a backflush cycle is not known, but perhaps the backflush causes slight redistribution of the wool fibers to create more HGMS sites. The ratio volume of feed treated to volume of backflush solvent is about five.

The backflush procedure was probably not capable of removing all the trapped particles, however, since a 0.120 MPa (20 psi) backpressure was developed by the matrix in the fourth cycle run. A large concentration of SRC particles was found at the initial portion of this matrix when it was removed from the canister. Particle buildup was not seen in matrices subjected to one cycle.

SEPARATOR PERFORMANCE MODEL

Scope and Development

The objective of modeling the separation process is to describe the breakthrough point of the separator, i.e., the capacity of the separator in terms of feed treated prior to performance degradation, as a function of the process parameters.

Three types of magnetic separator performances were consistently observed in all runs, and samples of each type are given in Figs. 5, 6, and 7. The first type, referred to as screening, is illustrated by the curves at the lower left-hand of Figs. 5 and 6. Here the applied magnetic field is zero, and the solids removal is due to the mechanical trapping of particles by the matrix.

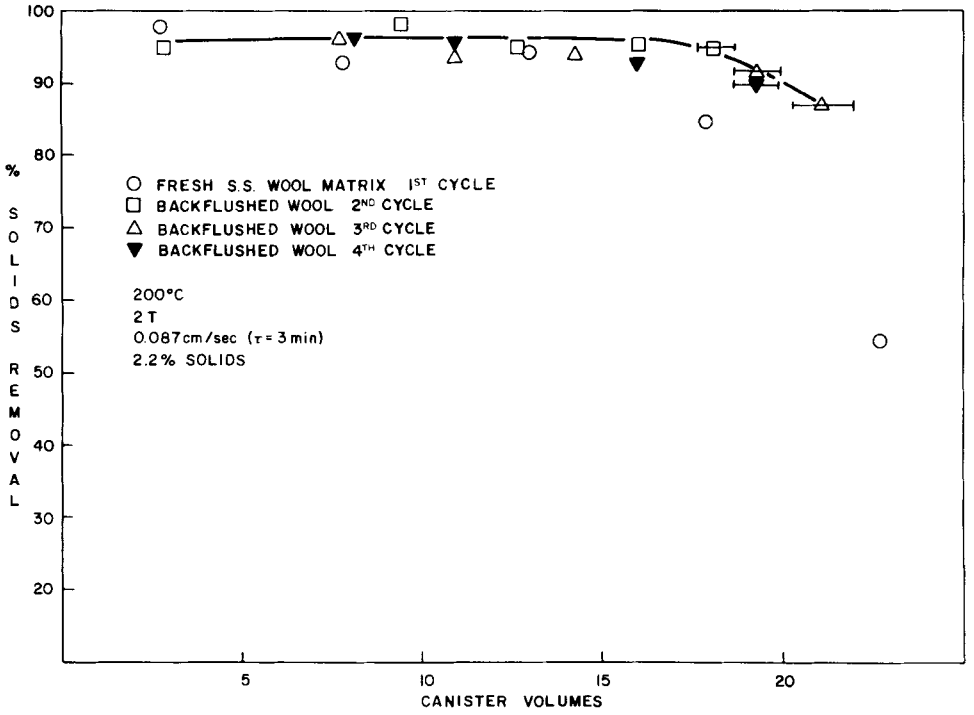

FIG. 16. Percent solids removal on fresh and backflushed matrices.

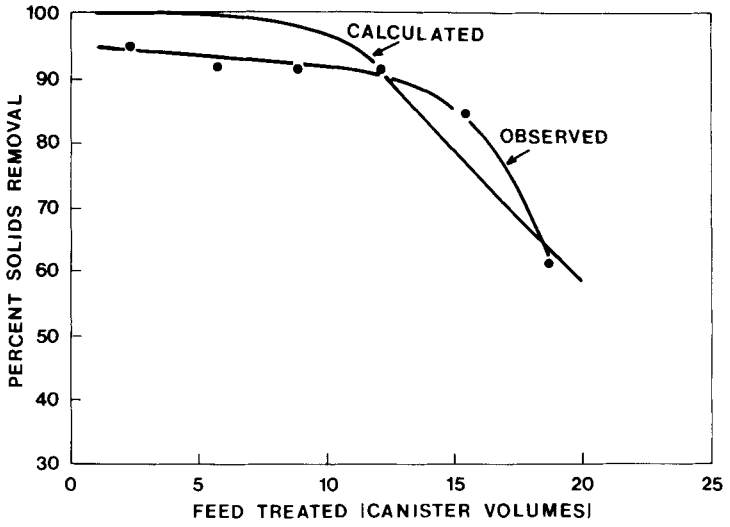

FIG. 17. Experimental and calculated percent solids removal vs volume of feed treated.

The second type of behavior is shown in the upper part of Fig. 1. This type of behavior, i.e., a slow decrease in solids removal with feed treated followed by a sharp decrease in removal with feed, is observed to occur in all runs where the residence time τ is greater than 1 min. The third type of behavior is illustrated by Fig. 7. Here no breakthrough point is observed. This type of curve is characteristic of runs in which the residence time is less than 1 min.

Consideration of the three types of separator performance indicates that optimum performance will occur when the applied field is nonzero and the residence time is greater than 1 min. In this situation, percent solids and ash removal will be approximately 90% or more for a larger amount of feed treated than in the other two cases. Consequently, the ensuing discussion will consider only these domains of values for the applied field and residence time.

Bean (*23*) has derived the following relationship for the performance of a high gradient magnetic separator:

$$\text{Fraction of magnetic particles removed} = 1 - \exp\left[\frac{-K_0 M_s d^2 \chi H \tau 1 - \varepsilon)\varepsilon}{D^2 \eta}\right] \qquad (1)$$

where K_0 is a geometrical constant, M_s is the saturation magnetization of the steel wool filaments, d is the magnetic particle diameter, χ is the magnetic particle's susceptibility, H is the magnitude of the applied field, τ is the feed residence time, ε is the fraction of space occupied by the matrix within the separator's active zone, D is the diameter of the gradient originating site on the matrix, and η is the viscosity of the feed.

The above relationship describes the separator performance for a situation vastly simpler than present in the removal of solids/ash from the SRC-I filter feed. For instance, the above assumes that the matrix is unloaded, i.e., the decrease in gradient originating sites as a function of feed treated is ignored. Rather than attempt to theoretically model this extremely complex separation process, a compromise had been sought in that the simplified theoretical model of Bean was empirically modified to fit the data base.

The following assumptions were invoked to simplify Eq. (1): (a) The effects of the particle diameter d, gradient originating site diameter D, susceptibility of SRC-I solids χ, saturation magnetization M_s of matrix fibers, and the geometric constant K_0 upon separation performance are identical for all runs. (b) The viscosity of the feed is inversely proportional to the temperature. (c) The void space $(1 - \varepsilon)$ is identical for all runs (i.e., actual value is within the range .86 to .88 for all runs). In addition, a term V_t denoting the amount of feed treated (expressed in canister volumes) is incorporated as a term in the denominator of the exponent. This is done to cause the percent solids, ash removal to vary inversely with the amount of feed treated.

The result is:

$$\text{Fraction of solids, ash removed} = 1 - \exp\left(\frac{-aH^b\tau^c T^d}{V_t^e}\right) \quad (2)$$

and the domains of the process variables are as follows: field H between 0.9 and 2.0 T, residence time τ between 1 and 6 min, temperature T between 150 and 245°C, and canister volumes of feed treated V_t greater than 1.0. These domains correspond to the region of optimal performance, as previously discussed. The empirical coefficients were determined by a nonlinear least-squares fit to be as follows: $a = 0.500$, $b = 1.172$, $c = 0.520$, $d = 0.600$, and $e = 1.952$.

Discussion

Figure 17 gives the results of Eq. (2) superimposed upon Fig. 5. This result was typical of those obtained for several runs using different process variable values. Initially, the calculated percent removal is greater than the observed, the calculated breakthrough point is less than the observed, and the calculated removal decreases to less then the observed as the amount of feed treated increases. It is to be noted that a third-order polynomial in the process variables did not significantly improve the fit.

The above results occurred with such regularity that it indicated a nonrandom bias (*24*) in the model. This nonrandom bias was corrected for by regressing the calculated breakthrough points upon the observed to yield a corrected breakthrough point. Table 1 and Fig. 18 present the results of the calculation. The numbers in the figure correspond to those in the table.

Figure 19 presents calculated corrected breakthrough points as a function

TABLE 1

Observed and Calculated Breakthrough Volumes[a]

Predicted breakthrough volume (canister volume)	Observed breakthrough volume (canister volume)	Observed % solids, ash removal at breakthrough point	Field (T)	Residence time (min)	Temperature (°C)
13.0 (1)	13.0	94	0.9	3.0	198
16.2 (2)	15.5	96	2.0	3.0	150
16.8 (3)	16.3	96	2.0	3.0	195
14.9 (4)	15.3	90	2.0	1.3	198
17.5 (5)	18.2	96	2.0	2.9	245
18.9 (6)	>19	>95	2.0	6.1	193
16.8 (7)	>16	>95	2.0	3.0	190

[a]The numbers within the parentheses in Column 1 correspond to the labeled points in Fig. 18.

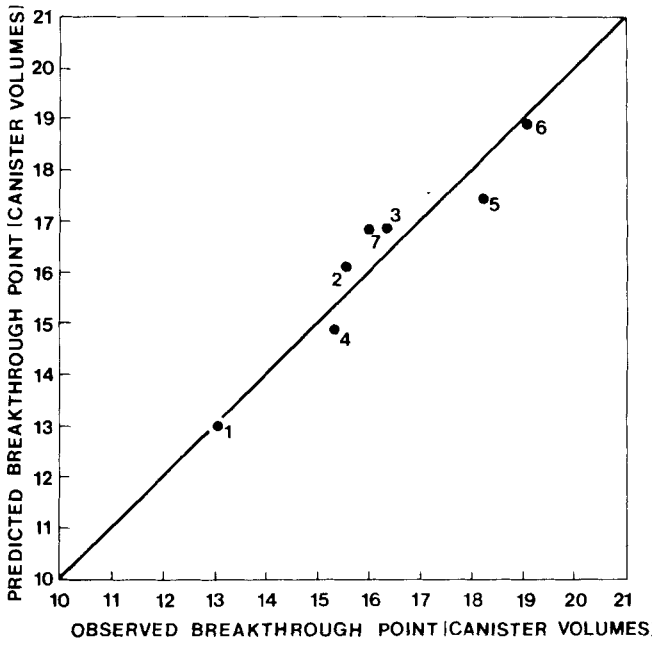

FIG. 18. Predicted breakthrough volume vs observed breakthrough volume. The numeric labels for the points correspond to entries in Table 1.

of residence time for values of temperature and field (sensitivity analysis). In this figure the breakthrough point occurs in all cases above 97% solids, ash removal. The figure illustrates, as do the data presented in Figs. 5 through 16, that separator capacity is increased with increasing values of temperature, residence time, and applied magnetic field.

Figure 19, the sensitivity analysis, also shows the relative importance of a change in the process variables upon separator capacity (i.e., increased breakthrough point at 97% solids, ash removal is identical to increased capacity). The magnitude of the applied field is the most important variable in this sense for an increase in the field results in a greater increase in separator capacity than occurs when increasing either the temperature or residence time. This greater capacity increases as the temperature or residence time increases. The sensitivity analysis also has implications for process optimization. For instance, the separator capacity is greater by 13% when the temperature is 250°C, the applied field is 1 T, and residence time is 6 min than when the variables have the values 150°C, 2 T, and 1 min, respectively. Here, the use of cost coefficients, if available, would permit selecting the better operating procedure.

Several runs were performed in which the residence time was less than 1

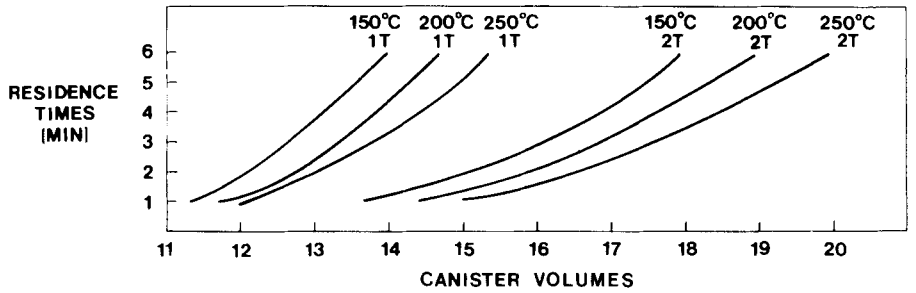

FIG. 19. Sensitivity analysis for breakthrough point.

min (e.g., Fig. 7). The breakthrough point was not observed in the runs and, therefore, it must be less than 2 canister volumes. Figure 19 is consistent with this observation for there is a rapid decrease in the breakthrough point as the residence time approaches 1 min. The curves give the appearance of being extrapolatable to a very low breakthrough point.

CONCLUSIONS

The properties of the Tacoma SRC-I filter feed are compatible for the removal of solids, including ash and inorganic sulfur, by HGMS. The particles in the feed possess a distribution of diameters which is approximately optimal for their magnetic removal by a stainless steel wool matrix.

The degree of filter feed particle removal by a high gradient magnetic separator increases with increasing values of the process variables, i.e., temperature, applied field magnitude, and residence time. The performance of the separator degrades with the amount of feed treated.

More specifically, as shown by the data presented, HGMS is capable of removing over 90% of the inorganic sulfur, solids, and ash from a diluted Tacoma SRC-I filter feed at feed velocities less than 0.17 cm/s (residence time 1.3 min), applied field 2.0 T, and temperature 190°C or greater. If the feed velocity is less than 0.04 cm/s (residence time 6 min), then the percent removal is over 97% for ash, 95% for inorganic sulfur and solids. Here, an HGMS feed of 1.9% solids and 1.2% ash yields an HGMS effluent of less than 0.10% solids and 0.036% ash, and more than 20 canister volumes of feed can be treated prior to separator performance degradation. The separator was regenerated 3 times without significant degradation of performance.

An empirical model developed to predict the separator capacity prior to separator performance degradation showed that the greatest increase in capacity occurs by increasing the magnitude of the applied field. Further-

more, this increased capacity itself increases as the temperature and/or residence time increases.

The HGMS results, when corrected by calculation for the dilution of the filter feed with process solvent in a 1:3 ratio, yield an HGMS effluent containing 0.14% ash. This value is based upon the assumption that the process solvent added as a diluent is identical to that in the process filter feed. Nonetheless, this result indicates a level of performance close to that of the rotary drum filter used in the SRC-I process. Consequently, the technical feasibility of utilizing a high magnetic gradient separator for solids/ash and inorganic sulfur removal in an SRC-I process has been indicated although its superiority to a rotary drum filter has not been demonstrated nor is to be implied.

REFERENCES

1. R. M. Jimeson, *Chem. Eng.*, p. 80 (March 1, 1976).
2. S. C. Trindade, PhD Thesis, Massachusetts Institute of Technology, 1973.
3. S. C. Trindade and H. H. Kolm, *IEEE Trans. Magn., Mag-9*, 310 (1973).
4. S. C. Trindade et al., *Fuel, 53*, 178 (1974).
5. H. H. Murray, *IEEE Trans. Magn., Mag-12*, 498 (1976).
6. F. E. Luborsky, *U.S. Bur. Mines, Rep. Invest. SRC-77-147* (September 1977).
7. Y. A. Liu, C. J. Lin, and D. M. Eissenberg, *Digests of the International Magnetics Conference*, Florence, Italy, May 1978.
8. C. J. Lin et al., *IEEE Trans. Magn., Mag-12*, 513 (1976).
9. Y. A. Liu and C. J. Lin, *Ibid, Mag-12*, 538 (1976).
10. Y. A. Liu et al., *Digests of the International Magnetics Conference*, Florence, Italy, May 1978.
11. Y. A. Liu and G. E. Crow, *Fuel, 58*, 345 (1979).
12. E. Maxwell, D. R. Kelland, and I. Y. Akoto. *IEEE Trans. Magn., Mag-12*, 507 (1976).
13. E. Maxwell, *EPRI Report AF-508*, August 1977.
14. I. S. Jacobs and L. M. Levinson, *Ibid.*, August 1977.
15. E. Maxwell and D. R. Kelland, *EPRI Report AF-875*, November 1978.
16. I. S. Jacobs and L. M. Levinson, *Ibid.*, November 1978.
17. E. Maxwell and D. R. Kelland, *IEEE Trans. Magn., Mag-14*, 482 (1978).
18. D. R. Kelland and E. Maxwell, International Conference on Industrial Applications of Magnetic Separations, Rindge, New Hampshire, July 1978. Proceedings To be Published.
19. J. A. Oberteuffer, *IEEE Trans. Magn., Mag-10*, 223 (1974).
20. R. R. Oder, *Ibid., Mag-12*, 428 (1976).
21. H. H. Kolm, U.S. Patent 3,676,337 (1972).
22. L. Petrakis, P. F. Ahner, and D. W. Grandy, To Be Published.
23. C. P. Bean, *Bull. Am. Phys. Soc. II, 16*, 350 (1971).
24. N. R. Draper and H. Smith, *Applied Regression Analysis*, Wiley, New York, 1966.

Received by editor January 26, 1981